Graphene mechanics: II. Atomic stress distribution during indentation until rupture

Supplementary Material

Bogdan I. Costescu,[a] and Frauke Gräter[ab]*

[a] *Heidelberg Institute for Theoretical Studies, Schloss-Wolfsbrunnenweg 35, 69118 Heidelberg, Germany*
[b] *CAS-MPG Partner Institute and Key Laboratory for Computational Biology, Shanghai Institutes for Biological Sciences, Chinese Academy of Sciences, 320 Yueyang Road, Shanghai 200031, China*
*E-mail: frauke.graeter@h-its.org

1 Calculation of atomic stress

Stress distribution in a material under mechanical load is often linked to material failure. The stress is typically defined in terms of force acting normal to a surface but, for in-plane stress in the single atom thick graphene sheet, the surface is ill-defined. We looked therefore into 3 ways of expressing stress to investigate its distribution in the graphene sheet during the indentation until rupture.

First, we used the definition of per atom punctual stress introduced by the Time-Resolved Force Distribution Analysis[1], which is computed as a sum of scalar pairwise forces and therefore expressed in units of force:

$$S_i = \sum_j |F_{ji}| \tag{1}$$

where S_i is the stress on atom i and F_{ji} is the atomic pairwise force between atom i and atom j. The calculation would yield a true pairwise stress if the force would be scaled by the inverse of the area through which individual atoms are subjected to the pairwise force. This area is not well defined, however, it can be considered constant throughout the sheet as graphene is a homogeneous material. Therefore, Equation 1 gives a valid representation of the in-plane stress in graphene, even though it uses units of force.

Secondly, from pairwise forces also obtained with TRFDA, we calculated the force acting across circles of increasing radii for which the center corresponds to the center of the graphene sheet. Each pair of atoms which are found on opposite sides of such a circle exert a normal force on the circle; summing up all these pairwise forces and dividing by the length of the circle results in a stress expressed as force over length, which we called *circular stress*. One could use the graphene thickness to turn these concentric circles into cylinders, which would recover the typical expression of stress as force over area. The definition of thickness for graphene is still controversial[2], but the thickness can be considered invariable throughout the sheet and would therefore appear only as a constant in circular stress calculations.

Thirdly, we calculated the virial atomic stress through an own implementation in GROMACS. For a set of interacting atoms found in a well-defined volume, the virial theorem relates the pressure to the temperature and the potential energy due to interactions between atoms. Similar to the implementation in LAMMPS[3], the virial atomic stress is expressed in units of force

times distance, or energy, over volume. The atomic volume is not well defined, but in a homogeneous material like graphene can be considered constant and omitted from stress calculations; thus, the virial atomic stress is expressed in units of energy. We used the von Mises formulation for the yield criterion to convert the tensor form of the virial atomic stress into a scalar value, representing the geometrical combination of normal and shear stresses acting on an atom.

In conclusion, these three definitions can be considered valid for graphene, even though they lead to absolute values of stress expressed in different units, which cannot be compared in a straightforward manner. Using each definition, we are able to compare the stress levels in the graphene sheet, allowing us to investigate the stress distribution throughout the sheet under indenter load. A scaling factor characteristic to each definition allows us to recover the typical expression of stress as force over area.

2 Kinetics of graphene sheet rupture

We assume a two state model for the graphene sheet rupture, with the intact sheet as reactant state and the ruptured sheet as product state. The two states are separated by an energy barrier $\Delta G^{\ddagger}$ along a reaction coordinate x, with $\Delta x^{\ddagger}$ being the distance between the reactant and product state along x. Using Arrhenius' law, we can define a reaction rate:

$$k_0 = Ae^{-\Delta G^{\ddagger}/k_B T} \tag{2}$$

where k_B is the Boltzmann constant and T is the temperature.

According to Bell's model[4,5], a constant force F, applied during the transition between states, performs work equal to $F\Delta x^{\ddagger}$, *i.e.* the free energy is linearly lowered by the force along x, resulting in a force-dependent reaction rate,

$$k = Ae^{-(\Delta G - F\Delta x^{\ddagger})/k_B T} \tag{3}$$

from which we can calculate a rate change by force according to

$$\frac{k}{k_0} = e^{F\Delta x^{\ddagger}/k_B T} \tag{4}$$

or

$$ln\ k \propto \frac{F\Delta x^{\ddagger}}{k_B T} \tag{5}$$

Thus, in Bell's model[4,5], the bond force is linearly dependent on the logarithm of the bond breaking probability, with a slope equal to $k_B T/\Delta x^{\ddagger}$. The same dependency is represented in Fig. 4c, and allows us to estimate $\Delta x^{\ddagger}$.

3 Raw indentation profiles

Each of the raw indentation profiles obtained from our simulations showed an initial jump to negative values shortly before the indenter touched the graphene sheet, similar to the snap-in observed in experiments (Fig. S3a in Ref. 6). This is a consequence of attractive Lennard-Jones interactions between some of the atoms of the two bodies and leads to a small deflection of the sheet towards the indenter; in experiments the indenter moved towards the sheet, in our MD simulations the sheet moved towards the indenter. This deflection is comparable in amplitude to the ripples which appear throughout the sheet due to thermal motions of the atoms[7], and therefore does not induce any significant change in the sheet geometry. Furthermore, we do not observe any shock waves forming and propagating through the sheet when the indenter comes into contact with it, which can also be explained by the presence of the ripples and the associated flexibility of the sheet. To obtain the correct force-displacement relationship, only the data from after the indenter tip has reached the initial position of the graphene sheet, equivalent to a cantilever becoming straight in an AFM experiment, is represented in Fig. 1a and S1 and used in calculations.

4 Movies

We note that the graphene dynamics after rupture, as represented in the final part of the movies, have not been included in the Results and Conclusions, as the truncated Morse potential can not be expected to yield chemically realistic scenarios for the rupture of these systems featuring strong electron conjugation.

Movie M1. Per atom punctual stress variation during indentation until rupture. Low level of background stress exists before the sphere touches the sheet. The stress increases significantly only in the area of graphene in contact with the sphere. Once a bond breaks, the material rupture evolves very fast and, for visualization purposes, the movie frames for this interval are shown with a 12.5 fold lower frequency than the rest.

Movie M2. Detailed view of the center of the graphene sheet during indentation until rupture, with atoms colored by punctual stress (compare Fig. 3a). Color scaling is different from Movie M1, showing only the variation in the range of high stress.

Movie M3. Detailed view on the center of the graphene sheet, with bonds colored by tensile force (compare Fig. 4b).

5 Figures

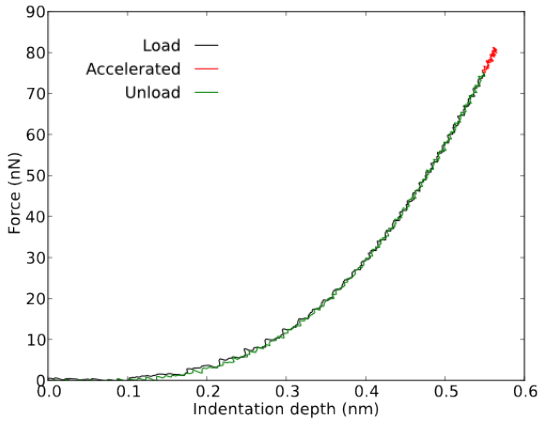

Fig. S1 Force-indentation profile with reverse load. Initial loading (black) was performed with a constant velocity of 0.01 nm ps^{-1}. The accelerated regime (red) was performed with an initial velocity of 0.01 nm ps^{-1} and an acceleration of -0.0001 nm ps^{-2}, for a total time of 200 ps. Unloading (green) was performed with a constant velocity of -0.01 nm ps^{-1}. A negative velocity denotes a movement of the sphere in the opposite direction, reducing the load on the graphene sheet.

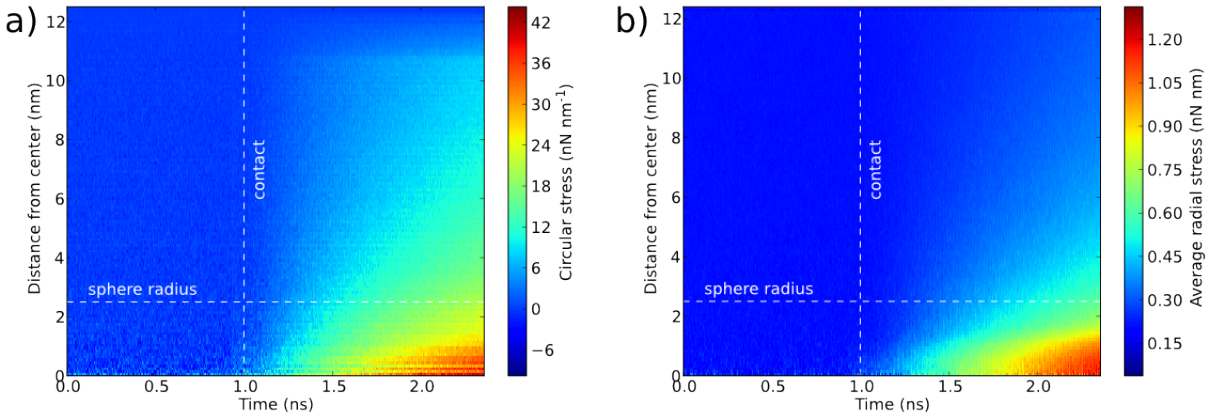

Fig. S2 Circular (a) and average radial virial (b) stress variation during indentation until rupture for a sphere radius of 2.5 nm, a graphene sheet radius of 12.5 nm and a sphere velocity of 0.01 nm ps^{-1}. The averaged radial virial stress was obtained by averaging the virial atomic stress over all atoms found at the same distance from the center of the graphene sheet. The distance from the center was computed with a resolution of 0.1 nm. Compare Fig. 3a for the averaged radial stress obtained from punctual stress for the same system.

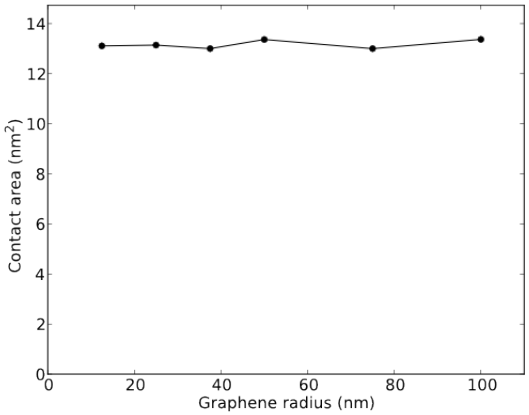

Fig. S3 Contact area between a sphere of 2.5 nm radius and graphene sheets of various radii less than 100 ps before rupture. Atoms are considered in contact if the distance between them is less or equal to 0.4 nm.

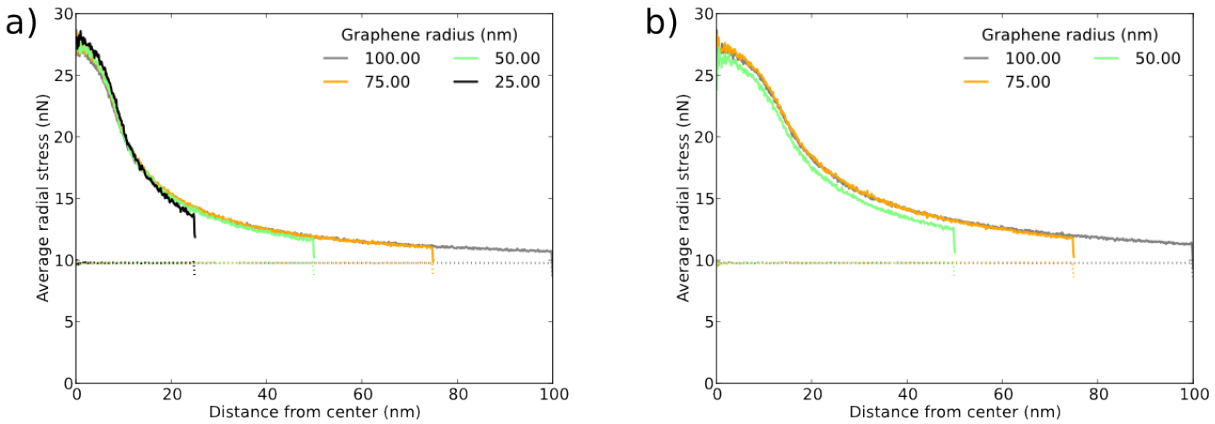

Fig. S4 Distribution of the average radial stress just before bond breaking for a sphere radius of 16.5 nm (a) and 27.5 nm (b) and several graphene sheet radii. The per atom punctual stress was averaged over all atoms found at the same distance from the center of the sheet. The distance from the center was computed with a resolution of 0.1 nm. Dotted lines show the background stress.

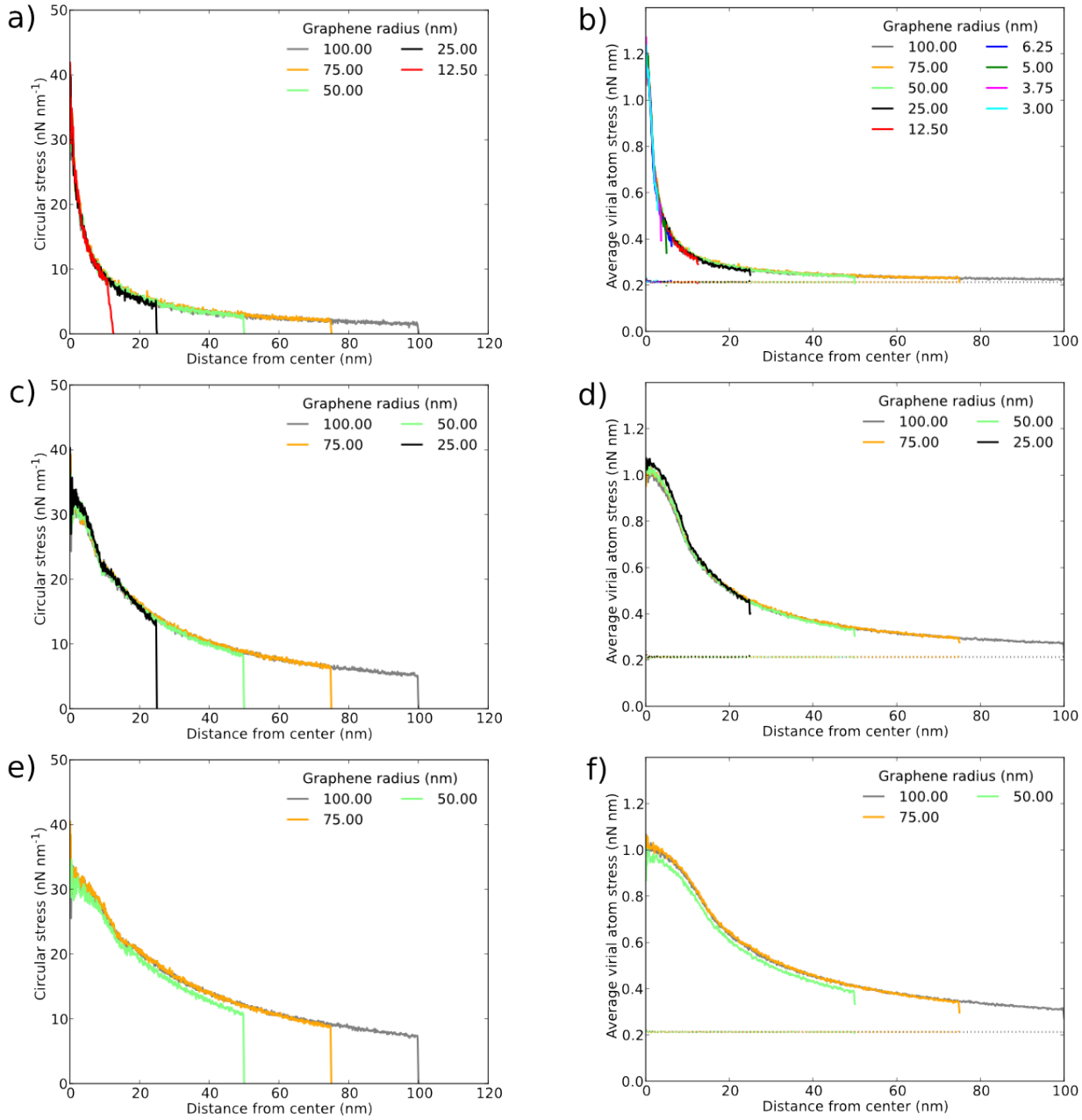

Fig. S5 Distribution of circular (a, c, e) and average radial virial (b, d, f) stress less than 100 ps before bond breaking for a sphere radius of 2.5 nm (a, b), 16.5 nm (c, d) and 27.5 nm (e, f) and several graphene sheet radii. The averaged radial virial stress was obtained by averaging the virial atomic stress over all atoms found at the same distance from the center of the graphene sheet. The distance from the center was computed with a resolution of 0.1 nm. Dotted lines show the background stress.

References

[1] B. Costescu and F. Gräter, *BMC Biophysics*, 2013, **6**, 5.
[2] F. Scarpa, S. Adhikari and A. S. Phani, *Nanotechnology*, 2009, **20**, 065709.
[3] A. P. Thompson, S. J. Plimpton and W. Mattson, *The Journal of Chemical Physics*, 2009, **131**, 154107.
[4] G. Bell, *Science*, 1978, **200**, 618–627.
[5] E. Evans and K. Ritchie, *Biophys J*, 1997, **72**, 1541–1555.
[6] C. Lee, X. Wei, J. W. Kysar and J. Hone, *Science*, 2008, **321**, 385–388.
[7] B. I. Costescu, I. B. Baldus and F. Gräter, *Physical Chemistry, Chemical Physics*, 2013, **99999**, 99999.